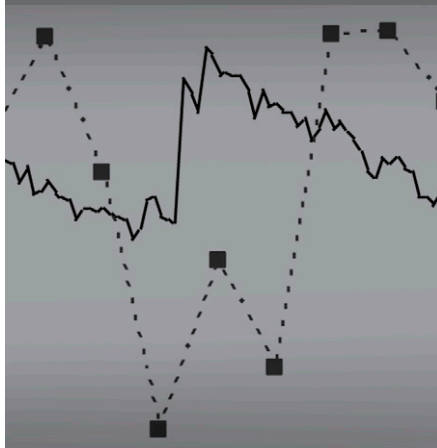X. Xiao
R. Horton*
T. J. Sauer
J. L. Heitman
T. Ren

Heat pulse sensors were used to measure cumulative soil water evaporation at different depths in a bare field. Results showed that heat pulse sensors were able to measure realistic soil water evaporation with depth and time during natural wetting and drying cycles.

X. Xiao and R. Horton, Agronomy Dep., Iowa State Univ., Ames, IA 50011; T.J. Sauer, USDA-ARS, National Lab. for Agriculture and the Environment, Ames, IA 50011; J.L. Heitman, Soil Science Dep., North Carolina State Univ., Raleigh, NC 27695; and T. Ren, Soil and Water Dep., China Agricultural Univ., Beijing, 100094 PRC. *Corresponding author (rhorton@iastate.edu).

Cumulative Soil Water Evaporation as a Function of Depth and Time

Soil water evaporation is an important component of the surface water balance and the surface energy balance. Accurate and dynamic measurements of soil water evaporation enhance the understanding of water and energy partitioning at the land–atmosphere interface. The objective of this study was to measure the cumulative soil water evaporation with time and depth in a bare field. Cumulative water evaporation at the soil surface was measured by the Bowen ratio method. Subsurface cumulative soil water evaporation was determined with the heat pulse method at fine-scale depth increments. Following rainfall, the subsurface cumulative evaporation curves followed a pattern similar to the surface cumulative evaporation curve, with approximately a 2-d lag before evaporation was indicated at the 3- and 9-mm soil depths, and several more days' delay in deeper soil layers. For a 21-d period in 2007, the cumulative evaporation totals at soil depths of 0, 3, 9, 15, and 21 mm were 60, 44, 29, 13, and 8 mm, respectively. For a 16-d period in 2008, the cumulative evaporation totals at soil depths of 0, 3, 9, 15, and 21 mm were 32, 25, 16, 10, and 5 mm, respectively. Cumulative evaporation results from the Bowen ratio and heat pulse methods indicated a consistent dynamic pattern for surface and subsurface water evaporation with both time and depth. These findings suggest that heat pulse sensors can accurately measure subsurface soil water evaporation during several wetting–drying cycles.

Abbreviations: BREB, Bowen ratio energy balance; DOY, day of the year.

As a key component of both the surface water balance and the surface energy balance, soil water evaporation impacts water and energy distributions at the land–atmosphere interface. Soil water evaporation is a dynamic process; however, many scientists have divided the process into three major stages (Hide, 1954; Lemon, 1956; Idso et al., 1974). The first stage is evaporation at the wet soil surface, which is controlled by atmospheric demand; the second stage is evaporation extending from the drying surface to the subsurface soil, which is controlled by upward water movement toward the soil surface; and the third stage is evaporation occurring below the surface where water vapor must diffuse through a dry surface layer to the atmosphere. The techniques for measuring soil water evaporation include energy balance (micrometeorology) and water balance approaches (Hanks and Ashcroft, 1980; Hillel, 1980). The Bowen ratio (Fritschen and Fritschen, 2005) and eddy covariance (Meyers and Baldocchi, 2005; Moncrieff et al., 1997) are widely used micrometeorological methods for estimating surface soil water evaporation over an adequate fetch area. The automatic weighing lysimeter method (van Bavel, 1961; Robins, 1965; Tanner, 1967), the manual weighing microlysimeter method (Boast and Roberston, 1982), and the soil water depletion method (Böhm et al., 1977) are established ways of determining evaporation by measuring changes in soil water storage and other components of the water balance. None of these methods can accurately measure dynamic soil water evaporation with time and depth in the field, however, especially at shallow depths near the soil surface. The reason they cannot measure soil water evaporation with depth and time is because they do not measure the millimeter-scale soil water moving up to the zone of evaporation. Based on sensible heat balance theory (Gardner and Hanks, 1966), Heitman et al. (2008a,b) developed a new heat pulse method to measure subsurface (3-mm depth and below) soil water evaporation with time at fine-scale depth increments in a bare field during an hourly time period. They reported that daily soil water evaporation from the heat pulse method agreed with the Bowen ratio and microlysimeter results. Comparisons of soil water evaporation among the three methods, however, have been limited to daily evaporation for a few discrete days. It is not yet known if the heat pulse method can be used to accurately measure evaporation with depth and time during an entire drying period following a rainfall event. There is a need to evaluate the ability of the heat pulse method to estimate soil water evaporation for consecutive days that represent wetting–drying sequences.

The objective of this study was to measure the surface and subsurface cumulative soil water evaporation with depth and time in a bare field including wetting–drying sequences. The cumulative evaporation from the soil surface was measured with the Bowen ratio method. The subsurface cumulative soil water evaporation was determined at fine-scale depth increments with the heat pulse method. The multi-day cumulative evaporation measurements were used to examine the development of a soil water evaporation zone with time and depth for natural wetting–drying processes in a bare field.

Materials and Methods
Experiment Location
The study was performed during the summers of 2007 and 2008 in a bare field (125 by 125 m) located near Ames, IA (41.98° N, 93.68° W). The soil at the site was a Canisteo clay loam (a fine-loamy, mixed, superactive, calcareous, mesic Typic Endoaquoll). The surface soil bulk density was 1.15 Mg m^{-3}. The soil consisted of 44% sand, 30% silt, and 26% clay, and the topography was relatively flat (slope <2%). This field was tilled each year and kept bare by spraying herbicides for weed control. Three-needle heat pulse sensors were installed to measure the subsurface cumulative soil water evaporation at several depth increments. About 20 m away from the heat pulse sensors, a Bowen ratio energy balance (BREB) measurement system was installed in this bare field to measure the surface cumulative soil water evaporation. The BREB system was positioned toward the northeast part of the field to optimize the fetch for the prevailing southwesterly winds. This provided fetch of approximately 100 m to the south, 130 m to the southwest, and 90 m to the west. The lower sensor was at 25 cm (top at 125 cm). Thus, fetch to upper sensor height ratios were approximately 80:1, 104:1, and 72:1 for winds from the south, southwest, and west, respectively.

Instrument Description and Installation
The heat pulse sensors used in this study were identical to those used by Ren et al. (2003) and Heitman et al. (2008a,b), which consisted of three parallel stainless steel needles (1.3-mm diameter, 40-mm length) with about 6-mm spacing between the needles. Each needle contained a chromel–constantan thermocouple for measuring temperature. In the middle needle there was also a resistance heater wire, through which a small current could be applied to generate a heat pulse, leading to temperature increases at the outer needles. The distances between neighboring needles were determined from heat pulse measurements made in agar-stabilized water (6 g L^{-1}) before experiments (Campbell et al., 1991).

Ten sensors at each of two locations were installed in the bare field each year to measure in situ subsurface cumulative soil water evaporation at several depths (Fig. 1). The two locations were within 20 m of each other. At each location, a narrow trench was dug, and the sensors were inserted at multiple depths into the undisturbed 0- to 40-mm soil layer. Heitman et al. (2008a,b) reported that evaporation was not detected at depths below 30 mm. The trench was carefully backfilled with soil. The heat pulse sensors were installed individually in 2007. To improve the accuracy of sensor placement depths, three sensors were glued together before installation in 2008. The thermocouples and heater wires of the heat pulse sensors were connected to multiplexers (AM16/32 and AM416, Campbell Scientific, Logan, UT), which were controlled by a Campbell CR10X datalogger. On the datalogger, the thermocouple reference was connected to single-ended Channel 1 (1H), excitation Channel 3 (E3), and an analog ground (AG). The datalogger was powered by a 12-V battery, which was recharged by a solar panel. Soil thermal diffusivity and volumetric heat capacity measurements were performed every 4 h. The measurement sequence for each heat pulse sensor consisted of a 30-s background temperature measurement, 8-s heating duration at the middle needle, and 72-s temperature measurements after heating, so the temperature response of a total time of 110 s with a 2-Hz sensing interval at the two outer needles and the power applied to the middle needle during the 8-s heating period was recorded in the sequence. The 30-s background temperatures were used to correct for temperature drift (Ochsner et al., 2006). In addition, the ambient soil temperature at each needle position was measured and recorded every 1 h.
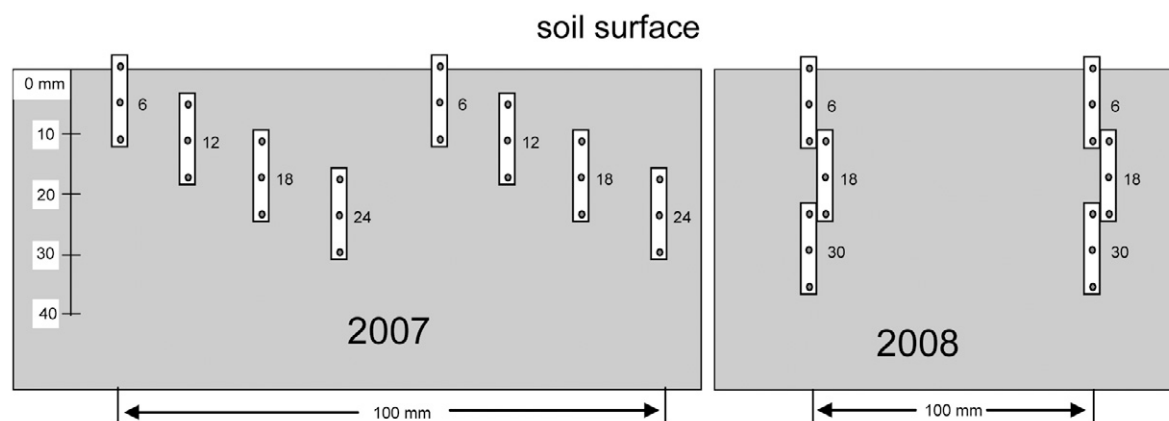

Fig. 1. A cross-sectional view of the heat pulse sensor installation designs in 2007 and 2008. White rectangles are the sensor bodies for the heat-pulse sensors; dark-colored circles within the rectangles indicate the position of sensor needles. Numbers beside each sensor indicate the middle needle depth (mm).

The BREB system used in this study was the same as that of Heitman et al. (2008b) and was similar to those of Bland et al. (1996) and Sauer et al. (2002). On a tripod, two air temperature–relative humidity probes (Model HMP45C, Vaisala Inc., Woburn, MA) with thermistor circuits were installed to measure the vapor pressure and air temperature. The sensors were mounted in aspirated radiation shields with a vertical separation of 1 m. Sensor elevation positions were exchanged every 5 min. On another tripod, a net radiometer (Model Q*7, Radiation and Energy Balance Systems, Seattle, WA) was installed at a height of 2 m. the soil heat flux was measured with two heat flux plates (Model HFT3.1, Radiation and Energy Balance Systems) at a depth of 60 mm. Soil temperatures at the 15- and 45-mm depths, adjacent to each plate, were measured with type T (copper-constantan) thermocouples. The measured soil temperature and estimated volumetric soil water content were used to determine energy storage changes in the soil above the flux plates (Sauer and Horton, 2005). All of the sensors were connected to a Campbell CR500 datalogger; data were collected at a 5-s interval and the 5-min averages computed. The BREB system provided estimates of net radiation, latent heat flux, sensible heat flux, and soil heat flux. A tipping bucket rain gauge was used to record rainfall.

Basic Theory of Heat Pulse Method

The theory for measuring soil water evaporation is based on the sensible heat balance of a soil layer (Gardner and Hanks, 1966; Heitman et al., 2008a,b). A heat pulse sensor can be used to measure the sensible heat balance terms for a soil layer, e.g., sensible heat in, sensible heat out, and the change in sensible heat storage (Fig. 2).

$$\left(H_u - H_l\right) - \Delta S = LE \tag{1}$$

where H_u and H_l are soil sensible heat fluxes (W m^{-2}) at the upper and lower boundaries, respectively, of a specified soil layer; ΔS (W m^{-2}) is the change in sensible heat storage of the soil layer; L (J m^{-3}) is the volumetric latent heat of vaporization; and E is the evaporation rate (m s^{-1}). For a specific soil layer, we assumed that the difference between the net sensible heat transferred and the change in sensible heat storage was equal to the latent heat. If the difference was positive, then some of the soil layer sensible heat was being partitioned to latent heat, indicating that some of the water in the soil layer was evaporating. If the difference was zero, then all of the soil layer sensible heat was accounted for, indicating that no water was evaporating and no water was condensing in the soil layer. If the difference was negative, then some of the soil layer sensible heat must have been deriving from latent heat as water vapor condensed and latent heat became sensible heat in the soil layer. Heat pulse measurements in conjunction with Eq. [1] were used to calculate the soil water evaporation, similar to the approach presented by Heitman et al. (2008a,b).
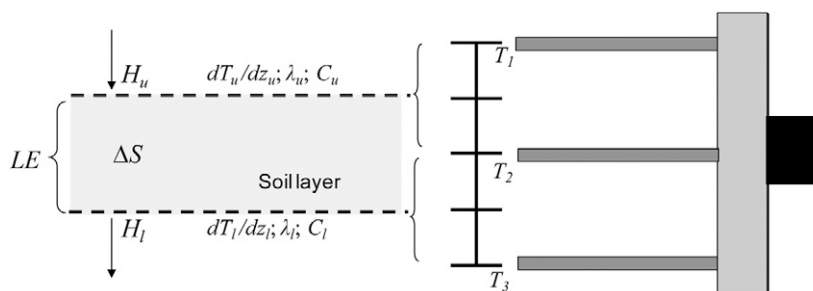

Fig. 2. Diagram of heat pulse sensor measurements applied to determine sensible and latent heat of a soil layer, where H is sensible heat flux, ΔS is the change in sensible heat storage, LE is latent heat, T is temperature, z is depth, λ is thermal conductivity, C is volumetric heat capacity, and the subscripts u and l represent upper and lower, respectively.

The temperature response with time at the outer needles of a heat pulse sensor to the heat pulse from the middle needle was used to determine the soil thermal diffusivity and soil volumetric heat capacity.

The soil thermal diffusivity (α, m^2 s^{-1}) was computed as (Bristow et al., 1994)

$$\alpha = \frac{r^2}{4t_m}\left(\frac{t_0}{t_m - t_0}\right)\left[\ln\left(\frac{t_0}{t_m - t_0}\right)\right] \tag{2}$$

where, for a given sensor, r (m) is the spacing between the middle and outer needle, t_0 is the heating duration (8 s), and t_m (s) is the time from the beginning of heating to when the maximum temperature occurred. Thermal diffusivities for the soil between the middle needle and the upper needle (α_u) and for the soil between the middle needle and the lower needle (α_l) were obtained from the outer needle temperature responses to the middle needle heat inputs for each heat pulse sensor.

The soil volumetric heat capacity (C, J m^{-3} °C^{-1}) was computed using (Knight and Kluitenberg, 2004)

$$C = \frac{q' t_0}{e\pi r^2 T_m}\left(1 - \frac{1}{24}\varepsilon^2 - \frac{1}{24}\varepsilon^3 - \frac{5}{128}\varepsilon^4 - \frac{1}{192}\varepsilon^5\right) \tag{3}$$

where T_m is the maximum temperature increase (°C), q' is the applied heating power per unit length of heater (W m^{-1}), and ε is the ratio of heating duration to the time corresponding to the maximum temperature increase ($\varepsilon = t_0/t_m$). The soil volumetric heat capacities for the soil between the middle needle and the upper needle (C_u) and for the soil between the middle needle and the lower needle (C_l) were obtained from the outer needle temperature responses to the middle needle heat inputs for each heat pulse sensor.

Accordingly, soil thermal conductivities (W m^{-1} °C^{-1}) from the middle needle to the upper needle (λ_u) and from the middle needle to the lower needle (λ_l) were computed as the product of α and C:

$$\lambda_u = \alpha_u C_u, \quad \lambda_l = \alpha_l C_l \qquad [4]$$

The temperature gradients (°C m^{-1}) dT_u/dz_u and dT_l/dz_l at the soil layer boundaries were determined from the measured ambient temperatures (T_1, T_2, and T_3, °C) and the calibrated distances (or depths, z, m) between the needles. Using λ_u and λ_l together with thermal gradients, the sensible heat fluxes (W m^{-2}), H_u and H_l, at the mid-depths of the adjacent needles were calculated with Fourier's law:

$$H_u = -\lambda_u \frac{dT_u}{dz_u}, \quad H_l = -\lambda_l \frac{dT_l}{dz_l} \qquad [5]$$

The change in sensible heat storage, ΔS, was calculated from the value of C (C is the average of C_u and C_l) and the middle needle temperature changes with time ($\Delta T_2/\Delta t$, °C s^{-1}) for a given soil layer with thickness Δz (m) (Ochsner et al., 2007):

$$\Delta S = C \frac{\Delta T_2}{\Delta t} \Delta z \qquad [6]$$

The latent heat of vaporization, L, for a given soil layer was calculated as a function of the middle needle temperature, T_2 (Forsythe 1964):

$$L = 2.49463 \times 10^9 - 2.247 \times 10^6 T_2 \qquad [7]$$

Soil thermal properties were calculated using Eq. [2–4], and sensible heat fluxes, changes in sensible heat storage, and latent heat distributions were calculated using Eq. [5–7]. Soil water evaporation rates were determined using Eq. [1]. In 2007, individual heat pulse sensors were installed in the soil to determine the soil water evaporation rates in the 3- to 9-, 9- to 15-, 15- to 21-, and 21- to 27-mm soil layers (see Fig. 3). In 2007, the soil water evaporation was calculated for each separate sensor. In 2008, to improve sensor depth accuracy, the heat pulse sensors were glued together before field installation. The 2008 heat pulse sensors were used to determine the soil water evaporation rates in the 3- to 9-, 9- to 15-, 15- to 21-, and 21- to 27-mm soil layers (see Fig. 3). Heat pulse measurements represented identical soil layers in 2007 and 2008. The reported evaporation values for each soil layer represent the average of replicated heat pulse measurements.

Evaporation rates were integrated over time to determine the cumulative evaporation for specific depths. The cumulative
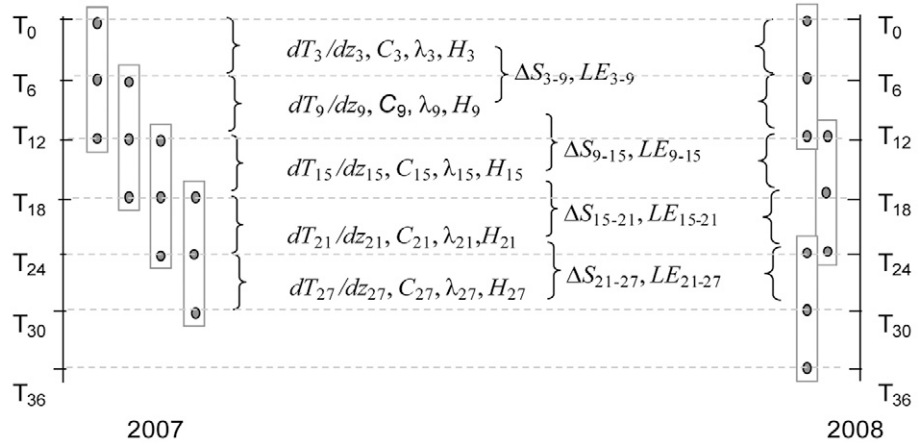

Fig. 3. The 2007 and 2008 heat pulse sensor placements used to calculate LE (latent heat). Each rectangular shape represents a three-needle heat pulse sensor, and the solid circles in the rectangles indicate the needle positions. In 2007, individual heat pulse sensors were inserted into the soil, and in 2008, to improve depth placement accuracy, heat pulse sensors were glued together before being inserted into the soil. The numeric subscripts indicate soil depth or soil layer (mm). The exact same depths and layers were represented in 2007 and 2008. The symbols in the diagrams refer to temperature (T), depth (z), volumetric heat capacity (C), thermal conductivity (λ), sensible heat flux (H), and change of sensible heat storage (ΔS).

evaporation at a specific depth is the sum of the evaporation rates for all of the soil layers below that depth, integrated over time. For example, the evaporation rate at the 3-mm depth is the sum of evaporation from the 3- to 9-, 9- to 15-, 15- to 21-, and 21- to 27-mm soil layers, and the cumulative evaporation is determined by integrating the evaporation rates over time.

◆ Results
Cumulative Soil Water Evaporation with Depth and Time

We obtained consecutive measurements for 21 d in 2007 and for 16 d in 2008. Figure 4 shows the volumetric soil water content for the 0- to 60-mm soil layer, the daily net radiation, the net cumulative evaporation at the 0-, 3-, 9-, 15-, and 21-mm soil depths, and the daily rainfall for the 2007 measurement period. Water content for the 0- to 60-mm soil layer represents the average water content of several soil layers measured by the heat pulse sensors. Because all of the measurements were made in a bare field, the cumulative evaporation from the Bowen ratio measurements included the net soil water evaporation occurring at and below the soil surface (0-mm depth). The cumulative evaporations at the 3-, 9-, 15- and 21-mm soil depths were measured by heat pulse sensors. During the measurement period, there were two rainfall events, day of the year (DOY) 172 through 173 and DOY 190.

Surface cumulative evaporation from the Bowen ratio method increased continuously during the 21-d measurement period. Following the first rainfall event (20 mm) on DOY 172 through DOY 173, cumulative evaporation at subsurface depths did not increase for 2 d. On the third day (DOY 176), the cumulative
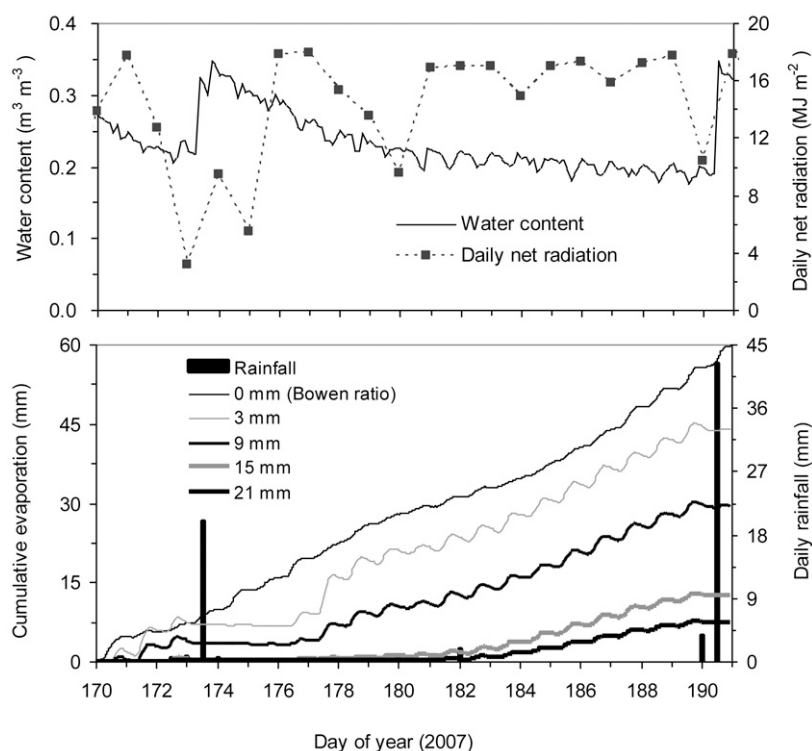
Fig. 4. The 2007 values for average soil water content (0–60 mm), daily net radiation, cumulative evaporation from the surface and at various subsurface soil depths, and daily rainfall.

evaporation from the Bowen ratio method increased continuously throughout the measurement period.

Following the first rainfall event (21 mm) on DOY 240 through DOY 241, cumulative evaporation at depths of 3, 9, 15, and 21 mm, with a time-lag pattern similar to the results from 2007, increased with time until the start of the second rainfall event (DOY 248). After DOY 243, the cumulative evaporation curve for the 3-mm depth began to parallel the surface cumulative evaporation curve until the second rainfall event from DOY 248 through 249. The cumulative evaporation curve for the 9-mm depth was further delayed to DOY 244 before it began to parallel the cumulative evaporation curves of the soil surface and 3-mm depth. The cumulative evaporation curves of the 15- and 21-mm depths behaved similarly, with only a few days' delay. Because there were only 2 d between the second and third rainfall events, no obvious increase in subsurface cumulative evaporation curves was noticed following the second rainfall event, indicating that the depth of evaporation shifted back to the soil surface. Similar to 2007, the cumulative evaporation at various soil depths in 2008 indicated the development of a soil water evaporation zone with time and depth. When the soil was wet following a rainfall, evaporation occurred first at

evaporation curve at the 3-mm depth began to increase. One day later, the cumulative evaporation curve at the 3-mm depth began to parallel the surface cumulative evaporation curve until the next rainfall event on DOY 190. The cumulative evaporation curves at the 9-, 15-, and 21-mm depths behaved similarly to the curve at the 3-mm depth, with a time lag of 1 d at the 9-mm depth and several days at the 15- and 21-mm depths. Cumulative evaporation curves at the various soil depths indicated the development of soil water evaporation zones with time and depth following a natural drying process in the bare field. In wet soil, soil water evaporation occurred at the soil surface and from the surface to a depth of 3 mm within 2 d after the rainfall event (i.e., first-stage evaporation). The zone of evaporation shifted downward to the 3- and 9-mm soil depths several days later, and even later to the 15- and 21-mm soil depths (i.e., the second and third stages of evaporation). Our results indicate that following rainfall, soil water evaporation is a continuous process not necessarily identified as having three separate stages.

In the summer of 2008, three rainfall events occurred in a 16-d period: DOY 240 through 241, DOY 248 through 249, and DOY 252 (Fig. 5). Surface cumulative
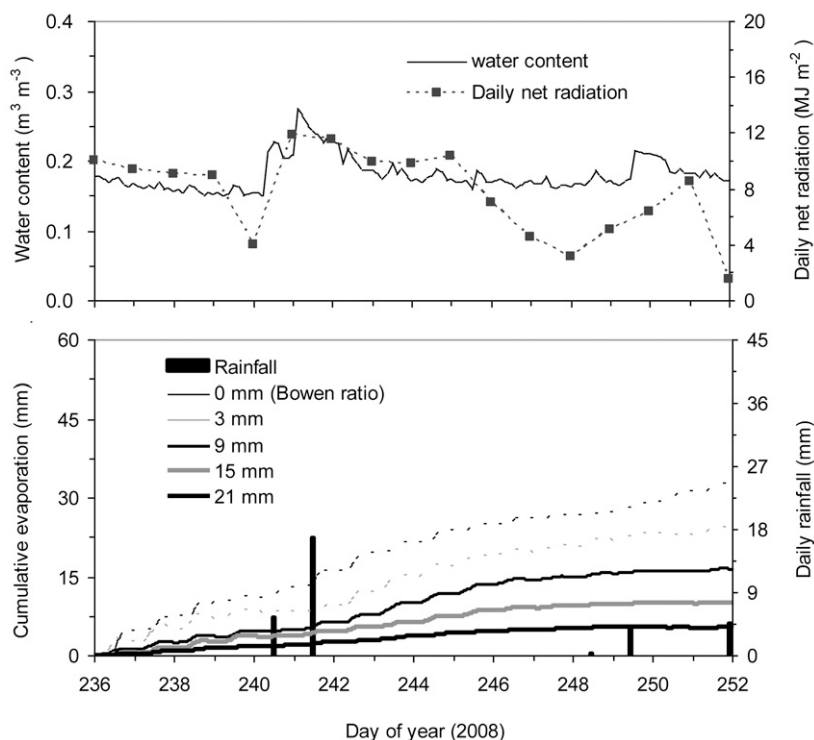

Fig. 5. The 2008 values for average soil water content (0–60 mm), daily net radiation, cumulative evaporation from the surface and at various subsurface soil depths, and daily rainfall.

the soil surface and then advanced from the surface to the shallow subsurface. When the soil surface started to dry, the evaporation zone shifted downward.

Cumulative evaporation curves for the soil surface from the Bowen ratio measurements and for the subsurface from the heat pulse measurements were consistent from year to year and depth to depth in both magnitude and time. This finding is particularly interesting because the measurement scales for the Bowen ratio and heat pulse methods differ considerably. Although both involve one-dimensional approximations, the Bowen ratio measurements occur above the ground surface and may be influenced by a land area of several hundred square meters, while the heat pulse sensors are buried below the soil surface and are influenced by the surrounding soil at a millimeter to centimeter scale. The data obtained from independent techniques representing different spatial scales had similar magnitude and were consistent for 2007 and 2008. For a 21-d period in 2007, the subsurface cumulative evaporation at soil depths of 3, 9, 15, and 21 mm from the heat pulse method was 44, 29, 13, and 8 mm, accounting for 73, 48, 21, and 13%, respectively, of the Bowen ratio surface cumulative evaporation (60 mm). For a 16-d period in 2008, the subsurface cumulative evaporation at soil depths of 3, 9, 15, and 21 mm was 25, 16, 10, and 5 mm from the heat pulse method, accounting for 74, 50, 30, and 16%, respectively, of the Bowen ratio result (32 mm). In both years, the results showed that the rate of cumulative evaporation decreased gradually from shallow to deeper soil.

Comparison between Years

The 2007 and 2008 measurement periods had similar amounts of rainfall (21 mm in 2007 and 22 mm in 2008). In the same bare field, however, the development of soil water evaporation from the soil surface to the subsurface occurred differently in 2007 and 2008. Part of the difference was associated with the temporal distribution of the rainfall and net radiation, and part was due to the differences in the initial soil water content. Other weather factors (such as air temperature and wind speed) were similar during the two measurement periods (data not shown).

For soil water evaporation, soil water is the source of water and net radiation is the main energy available for evaporation. In the days following rainfall events, the initial soil water content and net radiation at the soil surface differed between 2007 and 2008 (Fig. 4 and 5). The initial water contents of the 0- to 60-mm soil layers were about 0.21 and 0.17 m^3 m^{-3} before the first rainfall events in 2007 and 2008, respectively. The difference in initial soil water content was caused by the differences in the timing and amount of rainfall before the first measurement period rainfall event. The greater initial soil water content in 2007 than in 2008 was probably part of the reason for the larger evaporation rate in 2007 than in 2008. The mean daily surface evaporation for 7 d following the initial rainfall event was 2.8 mm in 2007 and 1.6 mm in 2008.

The first rainfall event in 2007 was 20 mm on DOY 172 through 173, and the daily net radiation totals for the following 2 d (DOY 174 and 175) were 9.5 and 4.5 MJ m^{-2}, respectively. The first rainfall event in 2008 was 22 mm on DOY 240 through 241, and the daily net radiation totals for the following 2 d (DOY 242 and 243) were 11.5 and 9.9 MJ m^{-2}, respectively. For the days following rainfall, the daily total net radiation was larger in 2008 than in 2007. Following the first rainfall event in 2007, there was almost no subsurface cumulative evaporation increase for the 2 d (DOY 174 and 175). Cumulative evaporation began to increase on DOY 176 at the 3-mm depth. In 2008, however, subsurface cumulative evaporation showed some increase shortly after the rain. These data indicate that net radiation affects the time lag of evaporation shifting from the surface to the subsurface following a rainfall event, which is physically consistent with the differences in energy available for depletion (evaporation) of soil water.

Additional future data observations may lead to the development of a quantitative expression of the time series of soil water evaporation following rainfall.

◆ Conclusions

Bowen ratio and heat pulse measurements of cumulative water evaporation from bare soil were consistent in magnitude and time. The cumulative evaporation clearly followed rainfall events, with the zone of soil water evaporation shifting from the surface downward. Cumulative evaporation with time showed the development of a soil water evaporation zone, revealing the time and depth dynamics of bare-field evaporation. The rates and the time lag of evaporation with depth were influenced by the initial water content and net radiation. The heat pulse method enabled the determination of cumulative evaporation during consecutive days and wetting–drying periods, and the heat pulse cumulative evaporation values were consistent with the Bowen ratio results.

References

Bland, W.L., J.T. Loew, and J.M. Norman. 1996. Evaporation from cranberry. Agric. For. Meteorol. 81:1–12. doi:10.1016/0168-1923(95)02304-6

Boast, C.W., and T.M. Roberston. 1982. A "micro-lysimeter" method for determining evaporation from bare soil: Description and laboratory evaluation. Soil Sci. Soc. Am. J. 46:689–696. doi:10.2136/sssaj1982.03615995004600040005x

Böhm, W., H. Maduakor, and H.M. Taylor. 1977. Comparison of five methods for characterizing soybean rooting density and development. Agron. J. 69:415–419. doi:10.2134/agronj1977.00021962006900030021x

Bristow, K.L., G.J. Kluitenberg, and R. Horton. 1994. Measurement of soil thermal properties with a dual-probe heat-pulse technique. Soil Sci. Soc. Am. J. 58:1288–1294. doi:10.2136/sssaj1994.03615995005800050002x

Campbell, G.S., C. Calissendorff, and J.H. Williams. 1991. Probe for measuring soil specific heat using a heat-pulse method. Soil Sci. Soc. Am. J. 55:291–293. doi:10.2136/sssaj1991.03615995005500010052x

Forsythe, W.E. 1964. Smithsonian physical tables. Publ. 4169. Smithsonian Inst.. Washington, DC.

Fritschen, L.J., and C.L. Fritschen. 2005. Bowen ratio energy balance method. p. 397–405. In J.L. Hatfield and J.M. Baker (ed.) Micrometeorology in agricultural systems. Agron. Monogr. 47. ASA, CSSA, and SSSA, Madison, WI.

Gardner, H.R., and R.J. Hanks. 1966. Evaluation of the evaporation zone in soil by measurement of heat flux. Soil Sci. Soc. Am. Proc. 30:425–428. doi:10.2136/sssaj1966.03615995003000040010x

Hanks, R.J., and G.L. Ashcroft. 1980. Applied soil physics. Springer-Verlag, New York.

Heitman, J.L., R. Horton, T.J. Sauer, and T.M. DeSutter. 2008a. Sensible heat observations reveal soil water evaporation dynamics. J. Hydrometeorol. 9:165–171. doi:10.1175/2007JHM963.1

Heitman, J.L., X. Xiao, R. Horton, and T.J. Sauer. 2008b. Sensible heat measurements indicating depth and magnitude of subsurface soil water evaporation. Water Resour. Res. 44:W00D05. doi:10.1029/2008WR006961

Hide, J.C. 1954. Observations on factors influencing the evaporation of soil moisture. Soil Sci. Soc. Am. J. 18:234–239. doi:10.2136/sssaj1954.03615995001800030002x

Hillel, D. 1980. Introduction to soil physics. Academic Press, London.

Idso, S.B., R.J. Reginato, R.D. Jackson, B.A. Kimball, and F.S. Nakayamaz. 1974. The three stages of drying of a field soil. Soil Sci. Soc. Am. J. 38:831–837. doi:10.2136/sssaj1974.03615995003800050037x

Knight, J.H., and G.J. Kluitenberg. 2004. Simplified computational approach for the dual-probe heat-pulse method. Soil Sci. Soc. Am. J. 68:447–449. doi:10.2136/sssaj2004.0447

Lemon, E.R. 1956. The potentialities for decreasing soil moisture evaporation loss. Soil Sci. Soc. Am. J. 20:120–125. doi:10.2136/sssaj1956.03615995002000010031x

Meyers, T.P., and D.D. Baldocchi. 2005. Current micrometeorological flux methodologies with applications in agriculture. p. 381–396. In J.L. Hatfield and J.M. Baker (ed.) Micrometeorology in agricultural systems. Agron. Monogr. 47. ASA, CSSA, and SSSA, Madison, WI.

Moncrieff, J., R. Valentini, S. Greco, G. Seufert, and P. Ciccioli. 1997. Trace gas exchange over terrestrial ecosystems: Methods and perspectives in micrometeorology. J. Exp. Bot. 48:1133–1142. doi:10.1093/jxb/48.5.1133

Ochsner, T.E., T.J. Sauer, and R. Horton. 2006. Field tests of soil heat flux plates and some alternatives. Agron. J. 98:1005–1014. doi:10.2134/agronj2005.0249

Ochsner, T.E., T.J. Sauer, and R. Horton. 2007. Soil heat storage measurements in energy balance studies. Agron. J. 99:311–319. doi:10.2134/agronj2005.0103S

Ren, T., T.E. Ochsner, and R. Horton. 2003. Development of thermo-time domain reflectometry for vadose zone measurements. Vadose Zone J. 2:544–551.

Robins, J.S. 1965. Evapotranspiration. p. 286–298. In C.A. Black et al. (ed.) Methods of soil analysis. Part 1. Agron. Monogr. 9. ASA, Madison, WI.

Sauer, T.J., and R. Horton. 2005. Soil heat flux. p. 131–154. In J.L. Hatfield and J.M. Baker (ed.) Micrometeorology in agricultural systems. Agron. Monogr. 47. ASA, CSSA, and SSSA, Madison, WI.

Sauer, T.J., P.A. Moore, J.M. Ham, W.L. Bland, J.H. Prueger, and C.P. West. 2002. Seasonal water balance of an Ozark hillslope. Agric. Water Manage. 55:71–82. doi:10.1016/S0378-3774(01)00185-8

Tanner, C.B. 1967. Measurement of evaporation. p. 534–574. In R.M. Hagen et al. (ed.) Irrigation of agricultural lands. Agron. Monogr. 11. ASA, Madison, WI.

van Bavel, C.H.M. 1961. Lysimetric measurements of evapotranspiration rates in the eastern United States. Soil Sci. Soc. Am. Proc. 25:138–141. doi:10.2136/sssaj1961.03615995002500020021x